

# Architected Lattice Materials with Tunable Anisotropy: Design and Analysis of the Material Property Space with the Aid of Machine Learning

Roman Kulagin,\* Yan Beygelzimer, Yuri Estrin, Artem Schumilin, and Peter Gumbsch

Architected beam lattice materials whose anisotropy can be tuned by varying the composition of their elementary cell are investigated. As an exemplary prototype of such material architecture, a regular triangular lattice with an elementary cell composed of 12 beams is considered. One out of three possible values of the elastic modulus is assigned to each beam. The structure is fully defined by a vector in the 12D composition-structure space whose components are given by the elastic modulus values of the beams comprising the elementary cell. The elastic properties of this 2D material are represented by the compliance elasticity tensor with six independent compliance coefficients. Aiming at a specific set of properties thus involves finding the point in the 12D composition-structure space that corresponds to a given point in the 6D property space. This is a problem of large dimensionality. To solve it, the neural network approach is used. This enables creation of architected materials with tunable elastic anisotropy. A chiral element combining large twist with additional anisotropy requirements is presented as an example of successful machine-learning-based optimization of beam lattices proposed.

anisotropic response of cells to various mechanical stimuli.<sup>[1,2]</sup> In engineering practice, materials with controlled anisotropy are used in various sensitive structures.<sup>[3]</sup> Directional dependence of the propagation velocity of acoustic waves stemming from the elastic anisotropy of the medium makes it possible to produce various materials and devices for breaking acoustic waves or damping of vibrations.<sup>[4]</sup> These are but a few illustrations of the significance of mechanical anisotropy.

Elastic anisotropy can be achieved in many ways. In composites, it is produced using a special arrangement of the constituents.<sup>[5]</sup> The paradigm of architected materials,<sup>[6,7]</sup> also referred to in the literature as hybrid materials, or metamaterials, and for brevity called archimats in the following, opens remarkable new possibilities for creating anisotropic properties. It builds on the idea of Ashby that the inner archi-

ture of a material can be regarded as an extra “degree of freedom” in materials design, which can be exploited to provide the material with desired properties.<sup>[8]</sup>


Some architected materials with artificially created mechanical anisotropy are already in existence; see the previous studies.<sup>[3,4,9,10]</sup> Among them, periodic beam lattice materials take

## 1. Introduction

Materials with anisotropic mechanical properties play an important role in nature and technology. Thus, many biomechanical processes in living organisms, which govern their growth, muscular activity, and oxygen and nutrient supply, are based on an

Dr. R. Kulagin, Prof. Y. Estrin  
Institute of Nanotechnology  
Karlsruhe Institute of Technology  
Hermann-von-Helmholtz-Platz 1, 76344 Eggenstein-Leopoldshafen,  
Germany  
E-mail: roman.kulagin@kit.edu

Prof. Y. Beygelzimer  
Donetsk Institute for Physics and Engineering named after A.A. Galkin  
National Academy of Sciences of Ukraine  
Nauki Ave., 46, 03028 Kyiv, Ukraine

 The ORCID identification number(s) for the author(s) of this article can be found under <https://doi.org/10.1002/adem.202001069>.

© 2020 The Authors. Advanced Engineering Materials published by Wiley-VCH GmbH. This is an open access article under the terms of the Creative Commons Attribution License, which permits use, distribution and reproduction in any medium, provided the original work is properly cited.

Correction added on 19 February 2021, after first online publication: The copyright line was changed.

DOI: 10.1002/adem.202001069

Prof. Y. Estrin  
Department of Materials Science and Engineering  
Monash University  
22 Alliance Lane, Clayton 3800, Australia

A. Schumilin  
Institute for Automation and Applied Informatics  
Karlsruhe Institute of Technology  
Hermann-von-Helmholtz-Platz 1, 76344 Eggenstein-Leopoldshafen,  
Germany

Prof. P. Gumbsch  
Institute for Applied Materials  
Karlsruhe Institute of Technology  
Straße am Forum 7, 76131 Karlsruhe, Germany

Prof. P. Gumbsch  
Fraunhofer Institute for Mechanics of Materials, IWM  
Wöhlerstraße 11, 79108 Freiburg, Germany

a special place due to the variability of properties they possess.<sup>[6]</sup> The properties are determined by the architecture of the elementary cell of the lattice. Commonly, it is the lattice geometry that is varied to achieve targeted characteristics of the material, while the properties of the beams are kept identical.<sup>[11,12]</sup> A further possibility of controlling the properties of lattice structures is using beams with two different values of stiffness.<sup>[13,14]</sup>

In this article, an alternative approach is proposed. It is based on varying the elastic properties of the beams in the unit cell while keeping the lattice geometry fixed. An important point is that the unit cell of the archimat is assumed to be larger than the unit cell of the geometric structure of the lattice itself. For example, in the case of a 2D triangular lattice, the geometric unit cell consists of three beams, whereas the unit cell of the proposed archimat is composed of 12 beams. This approach makes it possible to form more complex patterns by varying the stiffness of the beams, thereby enabling the control of the properties of the archimat. In practice, this can be realized, for instance, by 3D printing using several feed materials, or using beams with different cross-sectional dimensions. In the following we show, by considering the case of a regular triangular beam lattice, that this approach offers attractive prospects of developing archimats with controllable and tunable elastic anisotropy.

## 2. Structure and Properties of the Proposed Beam Lattice Archimats

The main idea behind the proposed beam lattice archimats is that the controllable anisotropy of their properties can be created by manipulating the number and arrangement of beams with different properties for a fixed geometry of the lattice they form. The idea is illustrated by considering an archimat with a regular triangular lattice as an example. It is known that such a lattice is elastically isotropic if all constituent beams have the same elastic modulus.<sup>[11]</sup> At the end of this section, it will be demonstrated that by putting together beams with different magnitudes of Young's modulus to a regular lattice, one can produce materials with various kinds of elastic anisotropy.

Consider a regular triangular lattice, which can be constructed by translation of an elementary cell consisting of 12 beams, as shown in **Figure 1a**. The "rule of the game" is that the elastic modulus of any beam can assume one of three possible values.

The architecture of the material under consideration is defined by a vector  $A$  in the 12D space of the stiffness coefficients of the beams of which the elementary cell is composed. The values of Young's modulus of the beams of the three types were taken as  $E_1 = 100$ ,  $E_2 = 60$ , and  $E_3 = 20$  MPa. Materials with such values can be obtained, e.g., by 3D printing using mixes of different polymers; see, e.g., the study presented in Chapter 9 of ref. [7]. An example of a particular realization of an archimat comprised by beams with different stiffness is shown in **Figure 1c**. The vector  $A$  for this archimat, after normalization of the components with respect to the largest elastic modulus ( $E_1$ ), is expressed as follows: (1;1;1;0.6;0.2;0.2;0.6;1;0.6;0.2;1).

Let us characterize our material in terms of the compliance elasticity tensor  $Z_{ijkl}$ , which connects the tensors of small elastic strain,  $\epsilon_{ij}$ , and stress,  $\sigma_{kl}$ <sup>[15]</sup>

$$\epsilon_{ij} = Z_{ijkl} \cdot \sigma_{kl} \quad (1)$$

For the 2D case we consider, the indices ( $i, j, k, l$ ) take the values (1, 2).

As the tensors  $\epsilon_{ij}$  and  $\sigma_{kl}$  are symmetrical, the equalities  $Z_{ijkl} = Z_{jikl} = Z_{ijlk}$  hold.<sup>[15]</sup> Furthermore, from the free energy minimum condition for an elastic solid, the relation  $Z_{ijkl} = Z_{klij}$  follows.<sup>[15]</sup> A corollary of these symmetry relations is that in a general 2D anisotropy case, only 6 out of the 16 components of the tensor  $Z_{ijkl}$  are independent. These components are  $Z_{1111}$ ,  $Z_{2222}$ ,  $Z_{1122}$ ,  $Z_{1112}$ ,  $Z_{2212}$ , and  $Z_{1212}$ . Their physical meaning is clear from Equation (1).

To relate the elastic properties of our lattice archimat to its composition, i.e., the number and arrangement of the beams of the three different kinds, we conducted Matlab calculations of elastic deformation of the lattice by the matrix method.<sup>[16]</sup> All nodes were assumed to be rigid. That is to say, elastic bending of the beams and the associated torques were considered. The dimensions of all beams (assumed to be square-shaped) were the same, with the length of 10 mm and the cross-sectional size of 1 mm × 1 mm. In the calculations, beam lattices containing 14 × 14 elementary cells were considered. The compliance of the overall structure was determined for three cases of loading: 1) extension along axis 1; 2) extension along axis 2; and 3) pure shear. Loading was simulated by applying to the nodes located at the outer contour of the structure forces  $f$  oriented such as to realize the above-mentioned three cases, **Figure 2**. The stress was calculated as

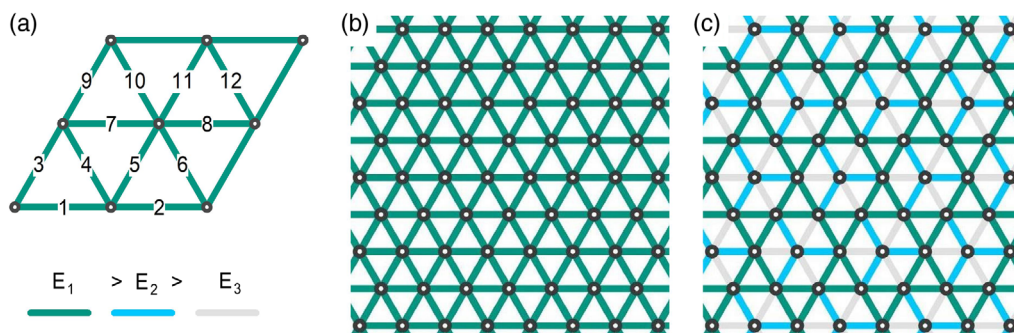


**Figure 1.** Schematics of an archimat with a regular triangular lattice formed by beams with different values of the elastic modulus. a) The structure of an elementary cell of the lattice. b) Example of a uniform lattice. c) Example of a specific realization of the lattice. The different colors of the beams indicate a difference in their Young's modulus,  $E$ .

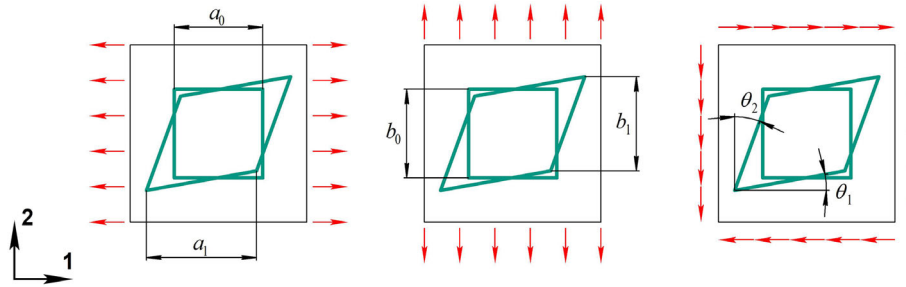


**Figure 2.** Schematic illustration of the three types of loading and the quantities used to determine stresses and lattice strains.

$$\sigma = \frac{N \cdot f}{L \cdot b} \quad (2)$$

where  $N$  is the number of nodes on one side of the contour of the lattice,  $L$  is the length of the side, and  $b$  is the beam thickness.

To determine the deformation of the lattice, while excluding possible boundary effects, a rectangle containing  $10 \times 10$  elementary cells was selected from within the  $14 \times 14$  array of cells considered. The magnitude of the force  $f$  was chosen, so that the resultant shape of the initial rectangle could be approximated by a parallelogram. This indicated the uniformity of the deformation of the lattice. The components of the strain tensor (for small deformations) were determined according to the following equations

$$\varepsilon_{11} = \frac{a_1 - a_0}{a_0}; \quad \varepsilon_{22} = \frac{b_1 - b_0}{b_0}; \quad \varepsilon_{12} = \frac{1}{2}(\tan \theta_1 + \tan \theta_2) \quad (3)$$

The designations  $a_0$ ,  $a_1$ ,  $b_0$ ,  $b_1$ ,  $\theta_1$ , and  $\theta_2$  are shown in Figure 2.

The components of the elastic compliance tensor  $Z_{ijkl}$  were calculated using the equations that follow from Equation (1)

$$\begin{aligned} Z_{1111} &= \frac{\varepsilon_{11}}{\sigma_{11}}; & Z_{2222} &= \frac{\varepsilon_{22}}{\sigma_{22}}; & Z_{1122} &= \frac{\varepsilon_{11}}{\sigma_{22}} \\ Z_{1112} &= \frac{\varepsilon_{11}}{\sigma_{12} + \sigma_{21}}; & Z_{2212} &= \frac{\varepsilon_{22}}{\sigma_{12} + \sigma_{21}}; & Z_{1212} &= \frac{\varepsilon_{12}}{\sigma_{12} + \sigma_{21}} \end{aligned} \quad (4)$$

Transforming them yields the elastic compliance tensor in the coordinate system rotated by an angle  $\varphi$  with respect to the initial one.<sup>[15]</sup> This enables plotting polar anisotropy diagrams for  $(Z_{1111}, Z_{2222}, Z_{1122}, Z_{1112}, Z_{2212}, Z_{1212})$ , whose radius in the  $\varphi$  direction is proportional to the respective compliance coefficient in the rotated coordinate system. In Figure 3, such diagrams are presented for four beam lattice materials with different inner architectures. The magnitude of the tensor components  $Z_{ijkl}$  is presented in a non-dimensional form as the product of the respective component and Young's modulus  $E_1$  of the stiffest of the three beam materials.

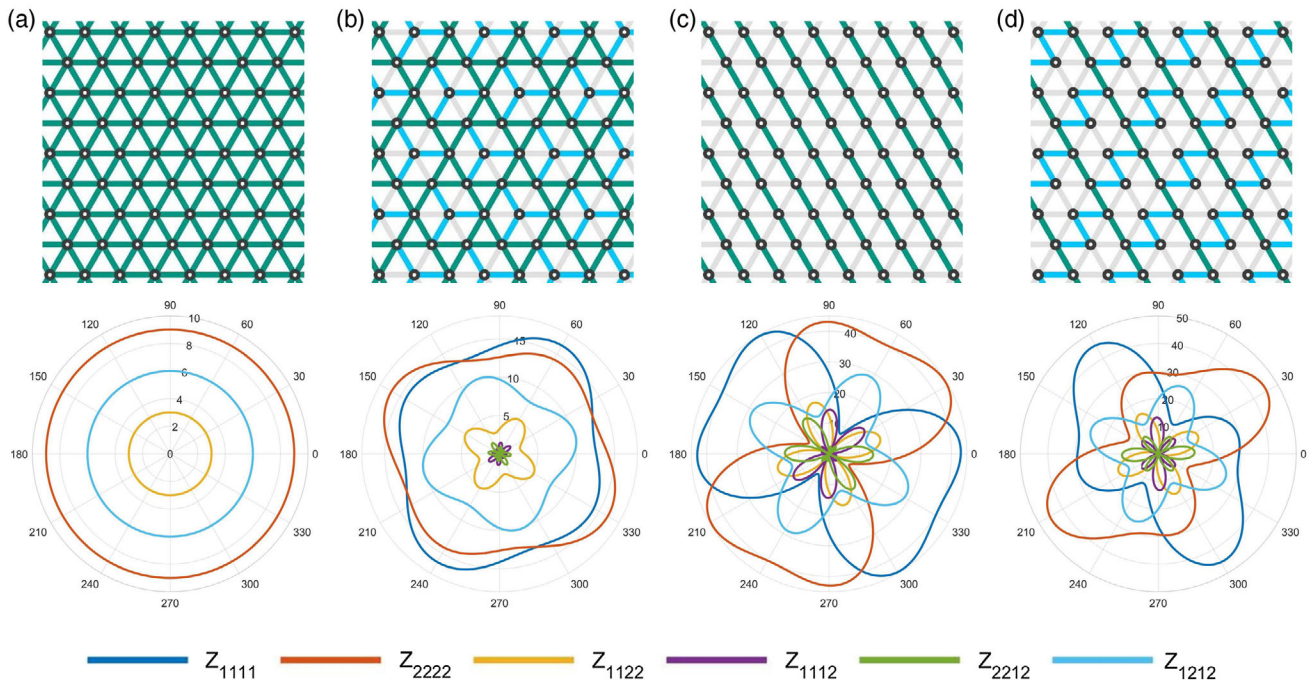


**Figure 3.** Anisotropy diagrams for the compliance coefficients in polar coordinates for four beam lattice materials with different compositions of the elementary cell. a) isotropic; b-d) anisotropic with various types of anisotropy.

The diagram in Figure 3a shows that a uniform lattice is elastically isotropic. The compliance coefficients  $Z_{1111}$  and  $Z_{2222}$  are equal, so that their diagrams are coincident, whereas  $Z_{1112}$  and  $Z_{2212}$  are zero. The non-dimensional Young's modulus  $E/E_1$  and shear modulus  $G/E_1$  and Poisson's ratio  $\nu$ , calculated for the isotropic materials using the well-known equations  $E/E_1 = (E_1 Z_{1111})^{-1}$ ,  $G/E_1 = (4E_1 Z_{1212})^{-1}$ , and  $\nu = -Z_{1122} Z_{1111}^{-1}$ ,<sup>[15]</sup> have the values  $E/E_1 = 0.114$ ,  $G/E_1 = 0.042$ , and  $\nu = 0.29$ . Within the accuracy of numerical computations, they are in good agreement with those obtained from the analytical expressions suggested by Ashby and co-workers for the parameter values used:  $E/E_1 = 0.115$ ,  $G/E_1 = 0.043$ , and  $\nu = 0.33$ .<sup>[11]</sup>

As seen from the diagrams, the materials whose architecture is shown in Figure 3b–d are elastically anisotropic. The archimats shown in Figure 3c,d exhibit a pronounced influence of the normal stresses  $\sigma_{11}$  and  $\sigma_{22}$  on the shear strain  $\varepsilon_{12}$ , as reflected in the magnitude of the components  $Z_{1112}$  and  $Z_{2212}$  of the elastic compliance tensor, which are referred to as the “coefficients of mutual influence.”<sup>[15]</sup> In Section 4, we will show how such archimats can be used to develop functional materials of the kind proposed by Wegener and co-workers.<sup>[13,17]</sup>

The above-mentioned analysis of Figure 3 shows that the variation of the makeup of the elementary cell of a regular triangle beam lattice can produce materials with different elastic anisotropies. This opens up a possibility of steering mechanical anisotropy through beam lattice design.

### 3. Exploration of the Material Property Space by Means of Machine Learning

In the way discussed in the foregoing section, one can ascribe a vector  $\mathbf{Z}(Z_{1111}, Z_{2222}, Z_{1122}, Z_{1112}, Z_{2212}, Z_{1212})$  in a 6D space to each vector  $\mathbf{A}$  describing the structure of the elementary cell in the 12D space. The possible sets of elastic properties of the entirety of the lattice archimats correspond to a certain region  $\Omega$  in the 6D space of the components of  $\mathbf{Z}$ . To design an archimat with desirable elastic properties, knowledge about the shape and boundaries of  $\Omega$  is necessary. It is obvious that obtaining such knowledge and its efficient use involves lengthy calculations and handling of a very large volume of data. Indeed, for an archimat with  $n$  beams in its elementary cell with  $k$  possible different types, there are  $N = k^n$  possible realizations of material architecture. If these structures were analyzed one-by-one, the number of realizations needed to gain sufficiently detailed information about the region  $\Omega$  would be on the order of  $k^n$ . In other words, the volume of the investigations grows exponentially with the number of beams in the elementary cell of an archimat. Problems related to exponential growth of the required volume of data with the number of governing parameters of the system are common to many research areas, such as adaptive control processes, probabilistic statistical image recognition, machine learning (ML), probabilistic classification, etc.<sup>[18]</sup> All these problems are fittingly described by the expression “a curse of dimensionality” that was coined by Bellman.<sup>[19]</sup>

There two aspects to the curse of dimensionality problem: 1) big data mining and 2) analysis of big data. The first aspect involves large expenditures in terms of time, labor, energy, etc. needed to gain large volumes of data. Thus, in the example

of archimats considered in the foregoing section ( $n = 12, k = 3$ ), there are  $N = 3^{12} = 531,441$  possible individual realizations of the material architecture. Of course, real experiments of this scale are out of the question, but even numerical simulations are extremely tedious and computationally costly, or practically impossible for larger  $n$  and  $k$ .

The second aspect of the curse of dimensionality is the problem of extracting regularities from massive volumes of big data. Again, the problem is common to all disciplines where it is not known which factors determine a certain phenomenon. In such a case, theoretical investigations need to be conducted, along with a large number of experiments, to unearth the governing factor (or factors) and study their effect. In the case of archimats, such studies are in their infancy. However, to provide a set of properties, which sometimes are antagonistic, an archimat should, in principle, be governed by multiple independent parameters. Therefore, the problem of extracting knowledge from massive volumes of big data is particularly acute for archimats.

Efficient methods aimed at overcoming both aspects of the curse of dimensionality have been developed in the context of ML.<sup>[20]</sup> The ML approach consists in developing a model for Big Data, whose parameters are identified based on statistical analysis of a limited selection of its realizations. A consequent enlargement of the volume of these selections leads to a gradual improvement of the model. This process is referred to as training of the model. A model trained in this way enables rapid generation of new data, which reduces the cost of resources required for obtaining the data. In this process, the ML methods make it possible to reveal patterns and regularities in Big Data, which helps reducing the dimensionality of the problem.

In this study, we used a Neural Network Fitting App by Matlab (Figure 4) to determine the region  $\Omega$ .<sup>[21]</sup>

As shown in Figure 4, we used a feed-forward network with two layers. In the output layer, linear neurons were used, whose number is determined by the dimension of the output data vector, in our case  $n_o = n_z = 6$ . In the hidden layer, sigmoid neurons were used, whose number was determined as  $n_h = \sqrt{n_i \cdot n_o} = \sqrt{12 \cdot 6} \approx 8$ .<sup>[22]</sup> The size of the training dataset for tuning the neural network should be 2 to 10 times greater than the total number of network tuning coefficients.<sup>[22]</sup> Considering that the network shown in Figure 5 has 158 coefficients and setting the size of the training dataset to be a fivefold of the number of the network tuning coefficients, we used 1000 realizations of beam lattice archimats for training. The network was trained using the Levenberg–Marquardt backpropagation algorithm. Finally, 1000 additional variants of various architectures were randomly calculated for testing the network. The training and testing results are shown in Figure 5.

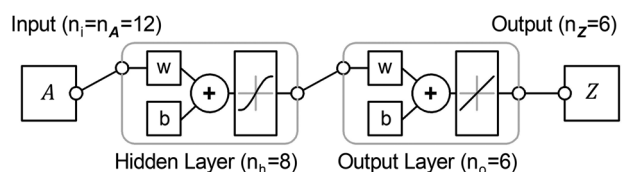


**Figure 4.** Schematics of the network architecture. Here,  $n$  (with a respective subscript) denotes the dimension of the vectors. (See the text for details.)

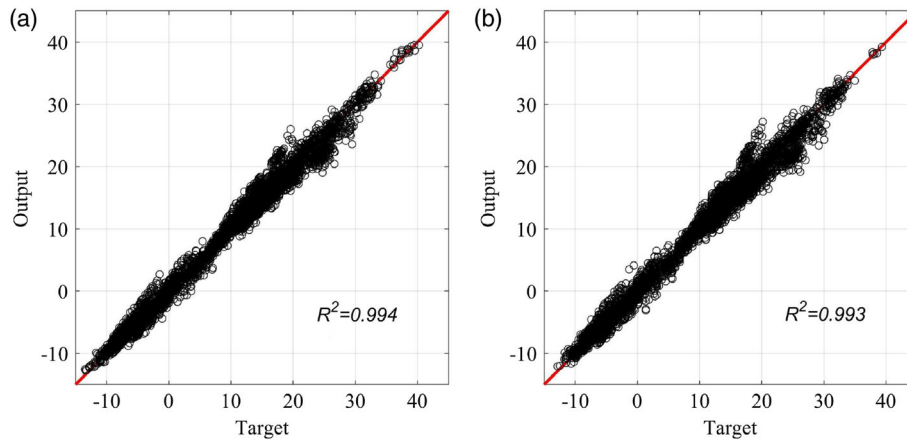


**Figure 5.** Results of a neural network fitting of archimat properties for a given architecture: a) training dataset and b) testing dataset.

Figure 5 displays data, which demonstrate a very good fit of the neural network results to those of the calculations. In this exercise, the time it took to calculate the compliance coefficients  $Z$  for a given architecture vector  $A$  was an order of magnitude shorter than that required for Matlab computations according to the method described in the previous section.

The trained network was used to determine the components of the elastic compliance tensor  $Z_{ijkl}$  for 20 000 variants of architecture of the beam lattice archimats. The results obtained are shown in **Figure 6** as points representing the properties of these archimats in planes whose coordinate axes correspond to pairs of independent compliance coefficients. These sets of points are 2D projections of the region  $\Omega$  of the material properties space. As mentioned earlier, ML methods are also effectively used to analyze big data. In our case, for the analysis of the data set calculated with the help of the network, we applied the method of clustering by the  $K$ -means.<sup>[21]</sup> The set presented in **Figure 6** is classed into six clusters ( $\Omega_1, \Omega_2 \dots \Omega_6$  highlighted in different colors), which agglomerate points with close values of the normalized compliance coefficients. The boundaries between the clusters are defined in such a way that the Euclidean distance of any point from the center of its own cluster is smaller than that from the center of any other cluster. The center of a cluster is the “center of mass” of all its points.

The 2D projections in **Figure 6** indicate some of the patterns inherent in the 2D archimats considered. In particular, a strong nearly linear correlation between the compliance coefficient  $Z_{2222}$  for loading along axis 2 and the shear compliance coefficient  $Z_{1212}$  attracts attention. Similarly, a nearly linear correlation between the coefficients  $Z_{1111}$  and  $Z_{1122}$  is observed. Owing to these linear correlations, some of the 2D projections of  $\Omega$  in **Figure 6**, for example,  $(Z_{1111}, Z_{2222})$  and  $(Z_{1111}, Z_{1212})$ , are similar.

Like Ashby’s Material Property Charts,<sup>[23]</sup> the 2D projections of  $\Omega$  can be of great help in a search for archimats with anisotropic elasticity required for a specific application. Indeed, the boundaries of the  $\Omega_1 \dots \Omega_6$  clusters immediately delineate and, thus, help visualizing, the domains formed by “collectives” of archimats whose inner makeup—however, different it might be—provides similar types of elastic response. In general, such

collectives cannot be identified intuitively, which demonstrates the crucial advantage offered by the neural network-based ML techniques.

#### 4. Discussion

The results reported earlier are a convincing demonstration that allowing for variability of the elastic characteristics of the beams on a lattice offers an efficient way to control the elastic anisotropy of beam lattice archimats. Even for a simple 2D version of such archimats with their elementary cells consisting of 12 beams, there exists a rather extended region  $\Omega$  in a 6D space of the compliance coefficients. This opens up new avenues for developing anisotropic plates and shells for use in structural members.<sup>[24]</sup> Of special interest are 2D adaptive systems whose functioning is associated with the existence of a set of stable states that are attained depending on the applied load.<sup>[25–27]</sup> This set is determined by the elasticity constants, notably by the compliance coefficients  $Z_{ijkl}$ . That is why an expansion of the region  $\Omega$  enables an extension of the set of possible stable states and, hence, the additivity of the structure. We consider this possibility of using the proposed archimats in plates and shells as very promising. It establishes a platform to design a structure and the material it uses in one go, and this synergy is beneficial to the design process.

Let us now turn to a different area where the archimats described earlier are believed to be promising as well. In the previous sections, we described the properties of the beam lattice archimats according to the traditional theory of anisotropic elasticity, which considers only the tensor of small deformations, i.e., symmetrical part of the displacement gradient  $\partial u_i / \partial x_k$ .<sup>[15]</sup> In general, the latter is represented as a sum of symmetrical and asymmetrical parts

$$\frac{\partial u_i}{\partial x_k} = 0.5 \left( \frac{\partial u_i}{\partial x_k} + \frac{\partial u_k}{\partial x_i} \right) + 0.5 \left( \frac{\partial u_i}{\partial x_k} - \frac{\partial u_k}{\partial x_i} \right) = \varepsilon_{ik} + \omega_{ik} \quad (5)$$

where  $\varepsilon_{ik}$  is the symmetric tensor of small deformations, and  $\omega_{ik}$  is the asymmetric rotation tensor.<sup>[28]</sup> For  $\partial u_i / \partial x_k \neq \partial u_k / \partial x_i$ ,  $\omega_{ik} \neq 0$  holds. Correspondingly,  $\theta_1 \neq \theta_2$  applies (see **Figure 2**),

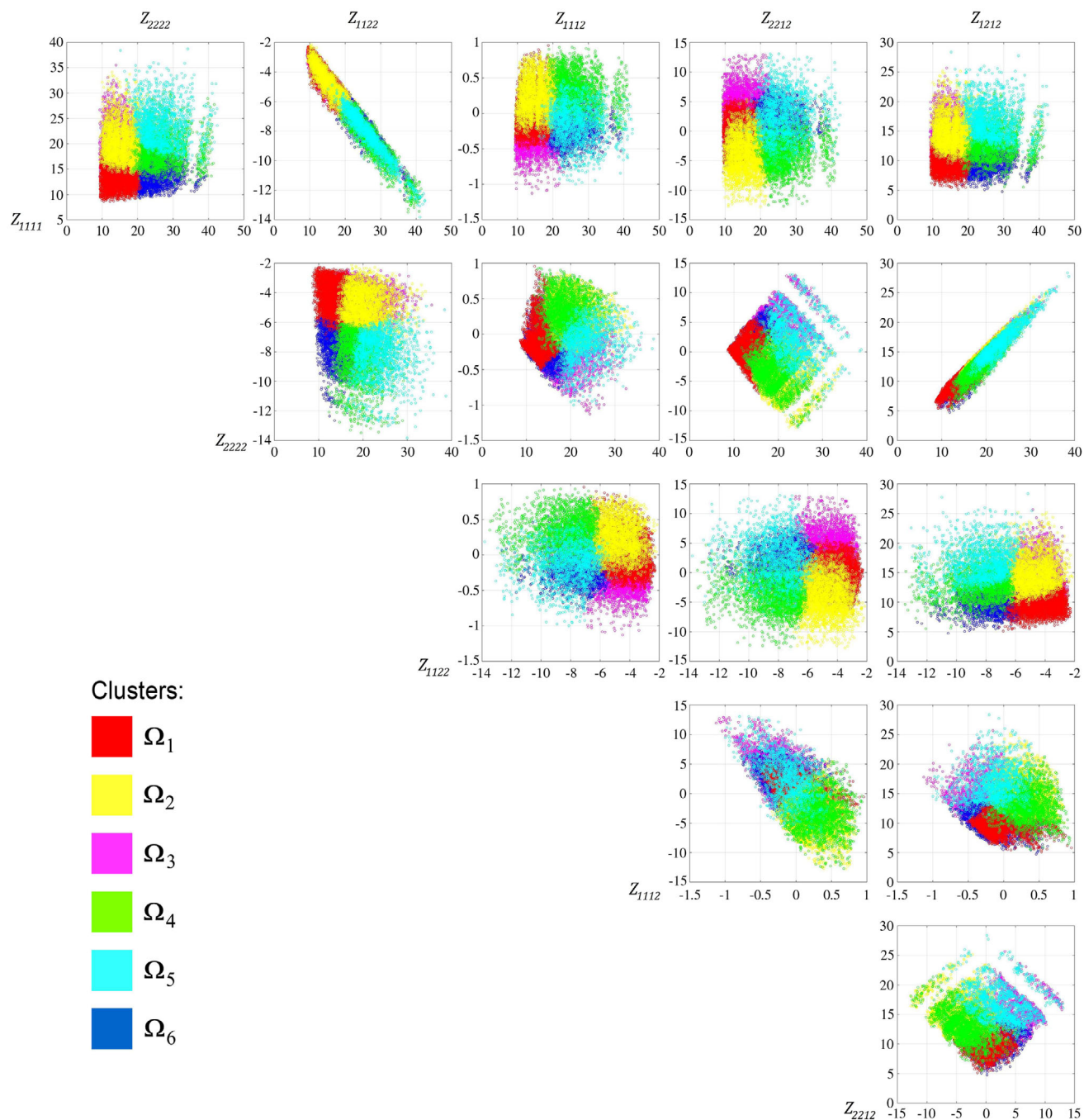


**Figure 6.** Projections of the representative points from within the region  $\Omega$  onto the compliance coefficient planes.

which can be used to tailor the interesting functional properties of materials associated with internal rotations.<sup>[28,29]</sup> Usually, the asymmetric theory of elasticity is used to characterize such effects quantitatively.<sup>[30]</sup> We will illustrate the effects of chirality qualitatively using, by way of example, a specific kind of a 3D lattice archimat that twists under compression/tension.

A material with such properties, referred to as a chiral mechanical metamaterial, was proposed and studied.<sup>[13]</sup> This material is composed of chiral and achiral elements, which are cube-shaped frames. The side faces of the chiral elements

have a special asymmetrical design. When an axial load is applied, the elements having such architecture twist, and as a result, the top and bottom bases of the elements rotate relative to each other. Chiral mechanical metamaterials are assembled in such a way that the chiral and achiral elements alternate.<sup>[13]</sup> This isolation of the chiral elements ensures that their twists do not obstruct and, hence, do not cancel, each other.

According to the proposed approach, a chiral 3D lattice archimat can be obtained if the side faces of 3D chiral elements are made from 2D beam lattices considered in the previous

sections.<sup>[13]</sup> This generates a specific kind of a 3D beam lattice archimat whose properties are fully defined by the elasticity parameters of the 2D lattice archimat.

The main requirement on the architecture of such a material is that twisting be produced when an axial load is applied. The principal advantage of the approach we propose is that a beam lattice archimat is multivariable, which makes it possible to satisfy additional requirements, as well. To that end, we use the Parameter Space Investigation Method together with the neural network introduced in the previous section.<sup>[21,31]</sup>

As already mentioned, the traditional theory of anisotropic elasticity does not consider rotations. Hence, strictly speaking, the considerations presented in Section 2 do not provide a basis for calculating rotations in the constituent 2D lattice archimats that determine the chiral properties of a 3D lattice archimat composed of them. We, therefore, estimate rotations qualitatively in that we assume that the inequality  $\theta_1 \ll \theta_2$  applies to a 2D archimat confined at the entire upper edge in direction 2 (Figure 2). In this case, it follows from the definitions of the quantities  $\varepsilon_{ik}$  and  $\omega_{ik}$  that  $\varepsilon_{12} = \omega_{12} = 0.5(\partial u_1 / \partial x_2)$  holds; see Equation (5). As a result, the magnitude of the simple shear strain of the 2D beam lattice archimat along axis 1 under loading applied along axis 2 is directly proportional to the compliance coefficient  $Z_{2212}$ . Accordingly, we will consider maximizing this parameter as the main design criterion. In general, there can be multiple criteria, each of them representing some important characteristic of the material, but in this example, we will restrict ourselves to only six components of the compliance tensor  $\mathbf{Z}$ . Let us denote the criteria by  $F_l(\mathbf{A})$ , where  $l$  is the criterion number, and  $\mathbf{A}$  is the vector that determines the arrangement of the beams in the elementary cell of the archimat (see Section 2). The parameter space investigation method works as follows. First, among all points of a specified set, it is necessary to determine the points  $\mathbf{A}_l$  where the criterion  $F_l$  reaches its optimum (smallest or largest) value  $F_{l0}$ . Such points are called “record holders” according to the respective criteria. Multi-criteria design is reduced to find the minimum of a complex criterion<sup>[31]</sup>

$$G(\mathbf{A}) = \sum_{i=1}^l \frac{\lambda_i}{\sum \lambda_i} \times \frac{|F_l(\mathbf{A}) - F_{l0}|}{F_{l0}} \quad (6)$$

where  $\lambda_i$  are weight coefficients reflecting the importance of the individual criteria.

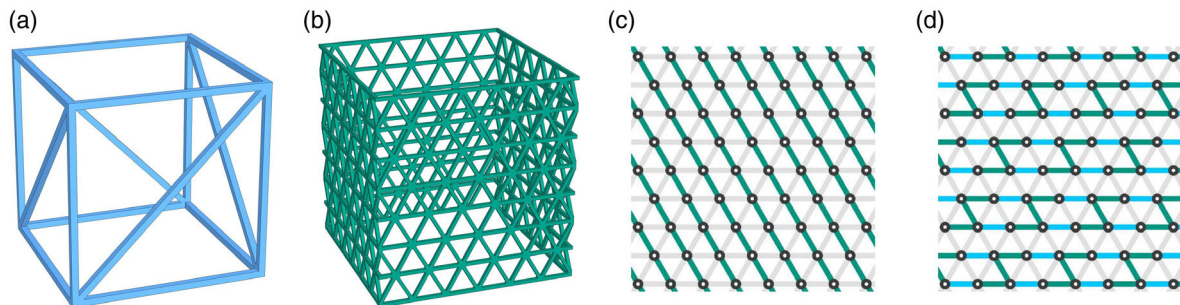


**Figure 7.** Examples of chiral element design: a) design from ref. [13] b) a beam lattice proposed in the present work, c) results of a single-criterion optimization of the structure of the faces of a cube, and d) results of multi-criteria optimization of the faces of a cube. The optimization criteria are defined in the text.

As mentioned earlier, in our case, the optimization criteria are six components of the compliance tensor, namely:  $F_1 = Z_{1111}$ ,  $F_2 = Z_{2222}$ ,  $F_3 = Z_{1122}$ ,  $F_4 = Z_{1112}$ ,  $F_5 = Z_{2212}$ ,  $F_6 = Z_{1212}$ . Thus, by setting the values of the weight factors  $\lambda_i (i = 1 \dots 6)$  and defining whether a maximum or a minimum of the  $i$ th criterion is sought ( $i = 1 \dots 6$ ), one can implement multi-criteria optimization according to Equation (6).<sup>[31]</sup> **Figure 7** shows the examples of the design of side faces of elementary cubes giving rise to chiral mechanical metamaterials. To calculate the optimal structures using a neural network, a full-factor numerical simulation was performed. For the first example of designed lattice archimat, we used the following vector  $\lambda = (0, 0, 0, 0, 1, 0)$ . For the archimat shown in **Figure 7c**, a single criterion was set as significant, and the corresponding condition was defined as  $F_5$  to attain the maximum possible value,  $F_5 \rightarrow \max$ . Its physical meaning is that a structure that would give the maximum shear along axis 1 when stretched (compressed) along axis 2 was sought. The identity of the structures shown in **Figure 7a,c**, as well as an intuitive understanding of their elastic response to axial loading, suggests an idea of how a chiral element can be designed as a beam lattice archimat.

Let us now consider a more complex example. For this version of a 2D lattice archimat, we use the following vector  $\lambda = (1, 1, 0, 1, 1, 1)$ . In this case, the following additional optimization conditions are set:  $F_1 \rightarrow \min$ ;  $F_2 \rightarrow \max$ ;  $F_4 \rightarrow \max$ ;  $F_5 \rightarrow \max$ ;  $F_6 \rightarrow \max$ . Such a material should be stiff in direction 1, soft in direction 2, bend as much as possible under axial load applied along axis 1 or axis 2, and be as compliant as possible when loaded by shear stresses. **Figure 7d** displays the structure of the beam lattice archimat sought for. Indeed, a careful visual analysis of this structure found using the above-mentioned ML approach shows that it fully complies with all optimization conditions. One would hardly expect that this pattern satisfying the above-mentioned multi-criteria requirements on the archimat could be identified without the aid of an ML technique.

The capabilities of the proposed archimats can be significantly expanded using beams with nonlinear elastic properties.<sup>[14,32]</sup> These can be pre-bent beams, which, therefore, have different stiffness in tension and compression, electrochemically activated beams, or temperature-sensitive beams.<sup>[33–35]</sup> Alternatively, non-linearity of the elastic response can be achieved by playing with the node construction (hinged/fixe).<sup>[36]</sup> In this case, the

properties of the archimat will also depend on the magnitude and direction of the load, which can be used for imparting to the archimat some desired functionalities.<sup>[33–36]</sup> Great opportunities can be expected from the application of the concept of programmable elastic metamaterials to the archimats introduced in this article.<sup>[37,38]</sup> The approach proposed in this article can also be applied for designing beam lattice patterns with a maximum tolerance to random defects arising during production.<sup>[39]</sup>

A further area where lattice archimats of the kind proposed can be expected to deliver improved properties is in structures designed for enhanced impact energy absorption, including core structures of sandwich panels. This will require optimization of the beam lattice architectures and the properties of the beam materials (of course, including their plasticity and fracture characteristics) targeting a maximum energy absorption.

By moving to 3D lattices, thus increasing the total number of beams involved, or by increasing the number of beams in the 2D elementary unit cell, the range of achievable material characteristics can be expanded. This, of course, would make optimal design much more complex. ML techniques will be indispensable in solving this problem. In this case, performing a full-factor experiment is obviously out of the question, and such ML tools as deep generative models can be the methodology of choice. Applying these, and other, ML techniques to design of complex beam lattice archimats will be the subject of the forthcoming work in this field.

## 5. Conclusion

The idea of designing lattice archimats with desired properties proposed here for the first time is based on the use of lattice patterns composed of beams with different elastic properties. The promising possibilities of implementing this idea in real structures were demonstrated by considering prototype 2D lattice archimats whose elementary cell consists of just 12 beams. The use of rigidly connected beams whose stiffness can have one of three different values on a triangular lattice enabled us to flexibly control the elastic properties of the lattice archimat. ML techniques were used to establish relations between the lattice archimat's patterns and its elasticity properties. As an example of a practical application, the design of a 3D chiral element with optimized properties suitable for use in chiral metamaterials was considered. The methodological framework developed in this work makes it possible to apply multi-criterion optimization in an efficient and computationally economical way. It can be concluded that by allowing the beams comprising a lattice archimat to possess more than just one value of Young's modulus provides an enormous richness of possible designs that may lead to novel materials and structures with new functionalities.

## Acknowledgements

P.G. acknowledges support from Deutsche Forschungsgemeinschaft (DFG) through the Excellence Cluster EXC 2082 "3D Matter Made to Order" (3DMM2O) and from the Fraunhofer Cluster of Excellence "Programmable Materials CPM."

## Conflict of Interest

The authors declare no conflict of interest.

## Keywords

architected materials, elastic anisotropies, lattice materials, machine learning

Received: September 11, 2020

Revised: October 4, 2020

Published online: October 23, 2020

- [1] D. Knudson, *Fundamentals of Biomechanics*, Springer, New York, NY **2007**.
- [2] H. Yi, Y. Chen, J. Z. Wang, V. M. Puri, Ch. T. Anderson, *J. Exp. Bot.* **2019**, *70*, 3561.
- [3] Y. Golfman, *Hybrid Anisotropic Materials for Structural Aviation Parts*, CRC Press, Taylor & Francis Group, New York, NY **2011**.
- [4] Y. K. Ahn, H. J. Lee, Y. Y. Kim, *Sci. Rep.* **2017**, *7*, 10072.
- [5] K. K. Chawla, *Composite Materials, Science and Engineering*, Springer, New York, NY **2019**.
- [6] M. F. Ashby, *Scr. Mater.* **2013**, *68*, 4.
- [7] Y. Estrin, Y. Brechet, J. Dunlop, P. Fratzl, *Architected Materials in Nature and Engineering. Archimats*, Springer Nature, Switzerland AG **2019**.
- [8] M. Ashby, *Acta Mater.* **1991**, *39*, 1025.
- [9] E. Barchiesi, M. Spagnuolo, L. Placidi, *Math. Mech. Solids* **2019**, *24*, 212.
- [10] W. Lee, D. Y. Kang, J. Song, J. H. Moon, D. Kim, *Sci. Rep.* **2016**, *6*, 20312.
- [11] N. A. Fleck, V. S. Deshpande, M. F. Ashby, *Proc. R. Soc. A* **2010**, *466*, 2495.
- [12] T. Maconachie, M. Leary, B. Lozanovski, X. Zhang, M. Qian, O. Faruque, M. Brandt, *Mater. Des.* **2019**, *183*, 108137.
- [13] P. Ziemke, T. Frenzel, M. Wegener, P. Gumbsch, *Extreme Mech. Lett.* **2019**, *32*, 100553.
- [14] M. Ryykin, V. Slesarenko, A. Cherkaev, S. Rudykh, *Philos. Trans. R. Soc.* **2019**, *378*, 20190107.
- [15] P. Vannucci, *Anisotropic Elasticity*, Springer, New York, NY **2018**.
- [16] O. C. Zienkiewicz, R. L. Taylor, *The Finite Element Method for Solid and Structural Mechanics*, Butterworth-Heinemann, Oxford **2013**.
- [17] T. Frenzel, M. Kadic, M. Wegener, *Science* **2017**, *358*, 1072.
- [18] A. Zimek, E. Schubert, H.-P. Kriegel, *Stat. Anal. Data Min.* **2012**, *5*, 363.
- [19] R. E. Bellman, *Adaptive Control Processes: A Guided Tour*, Princeton University Press, Oxford **1961**.
- [20] N. J. Nilsson, *Principles of Artificial Intelligence*, Morgan Kaufmann Publishers Inc., Burlington, MA **1986**.
- [21] Matlab, <https://www.mathworks.com/products/matlab.html> (accessed: October 2020).
- [22] T. Masters, *Practical Neural Network Recipes in C++*, Academic Press Limited, London **1993**.
- [23] M. F. Ashby, *Materials Selection in Mechanical Design*, Butterworth-Heinemann, Oxford **1999**.
- [24] R. M. Jones, *Mechanics of Composite Materials*, Taylor & Francis, New York **1999**.
- [25] F. Mattioni, P. M. Weaver, K. D. Potter, M. I. Friswell, in *Proc. 16th International Conference On Adaptive Structures and Technologies*, Destech Publications Inc, Paris **2006**.
- [26] P. M. Sobota, K. A. Seffen, *R. Soc. Open Sci.* **2019**, *6*, 190888.



- [27] G. Arena, R. M. Groh, A. Brinkmeyer, R. Theunissen, P. M. Weaver, A. Pirrera, *Proc. R. Soc. A* **2017**, 473, 20170334.
- [28] H. Bahaloo, Y. Li, *J. Appl. Mech.* **2019**, 86, 041002.
- [29] Y. Jiang, Y. Li, *Adv. Eng. Mater.* **2017**, 19, 1770023.
- [30] W. Nowacki, in *Micropolar Elasticity, International Centre for Mechanical Sciences (Courses and Lectures)* (Eds: W. Nowacki, W. Olszak) Springer, Vienna **1974**.
- [31] R. Statnikov, A. Statnikov, *The Parameter Space Investigation Method Toolkit*, Artech House, Inc., London **2011**.
- [32] S. Kamrava, R. Ghosh, Z. Wang, A. Vaziri, *Adv. Eng. Mater.* **2018**, 21, 1800895.
- [33] K. Bertoldi, V. Vitelli, J. Christensen, M. Van Hecke, *Nat. Rev. Mater.* **2017**, 2, 17066.
- [34] X. Xia, A. Afshar, H. Yang, C. M. Portela, D. M. Kochmann, C. V. Di Leo, J. R. Greer, *Nat.* **2019**, 573, 205.
- [35] H. Zhu, T. Fan, Q. Peng, D. Zhang, *Adv. Mater.* **2018**, 30, 1705048.
- [36] M. Shaat, A. Wagih, *Sci. Rep.* **2020**, 10, 2228.
- [37] B. Haghpanah, H. Ebrahimi, D. Mousanezhad, J. Hopkins, A. Vaziri, *Adv. Eng. Mater.* **2015**, 18, 643.
- [38] L. Jin, A. E. Forte, B. Deng, A. Rafsanjani, K. Bertoldi, *Adv. Mater.* **2020**, 32, 2001863.
- [39] D. Pasini, J. K. Guest, *MRS Bull.* **2019**, 44, 766.